A Comparison of OFDM and GFDM-based MFSK Modulation Schemes for Robust IoT Applications

Ghaith Al-Juboori, Evgeny Tsimbalo, Angela Doufexi and Andrew R. Nix
Communication Systems and Networks Group-Department of Electrical and Electronic Engineering
University of Bristol, Bristol, United Kingdom.
Email: Ghaith.al-juboori, e.tsimbalo, a.doufexi, Andy.nix@bristol.ac.uk

***Abstract*—Orthogonal Frequency Division Multiplexing based M-ary Frequency Shift Keying (OFDM-MFSK) is a non-coherent modulation scheme that was proposed for robust transmission over fast fading environments. It combines the MFSK modulation scheme with OFDM. In this paper, the Generalized Frequency Division Multiplexing (GFDM) waveform is considered to use with MFSK to take the advantages of the low out of band radiation and relaxed synchronisation requirements. Different methods to combine MFSK and GFDM are proposed and their performances are evaluated and compared with OFDM-MFSK. The mixed sub-carrier and sub-symbol method, which is one of the proposed methods, is the most promising technique. Additionally, gain margin is also seen for MFSK modulation scheme compared to ordinary OFDM or GFDM. This gain can be used to radically improve the performance for some 5G applications, such as IoT, at low Signal to Noise Ratio (SNR) values.**

Keywords*—GFDM, OFDM-MFSK, GFDM-MFSK, Non-coherent detection.

I. Introduction

Channel estimation is an important issue in certain wireless communication systems operating in fast fading environments such as high speed trains applications [1]. Non-coherent modulation schemes can be used to provide robust transmission in these applications. OFDM based MFSK (OFDM-MFSK), which is the combination of non-coherent detection for M-ary Frequency Shift Keying (MFSK) and Orthogonal Frequency Division Multiplexing (OFDM) transmission, was proposed and analysed in [2]. This combination leads to very modest receiver structure without any need for equalisation and channel estimation.

Some IoT applications in 5G, such as smart meters, need to operate in low signal strength conditions since they are installed in basements of buildings. Moreover, the information which they need to exchange with the network is very low [3]. Therefore, OFDM-MFSK is one of the promising solutions for these applications.

OFDM has great features that enable it to be used in many applications and standards such as its robustness to Inter Symbol Interference (ISI) and its simple implementation due to the use of the Fast Fourier Transform (FFT) algorithms [4]. However, OFDM suffers from many drawbacks, for example, its high Out-Of-Band (OOB) radiation, its sensitivity to the time and carrier frequency synchronization and its high Peak to Average Power Ratio (PAPR) [5].

In this paper, we investigate using the Generalized Frequency Division Multiplexing (GFDM) waveform, which is one of the important candidates for the 5G waveform, with the MFSK modulation. GFDM has considerable features such as low OOB radiation because of the filtering process at each sub-carrier, better spectral efficiency due to a single Cyclic Prefix (CP) for the GFDM block, which consists of multiple sub-symbols, and its simple synchronization requirements [6]. Different methods to combine GFDM and MFSK have been proposed and the performances of both GFDM based MFSK (GFDM-MFSK) and OFDM-MFSK have been evaluated and compared in different channel types.

The remainder of this paper is arranged as follows: Section II gives a brief description of the GFDM air interface and OFDM-MFSK and its transceiver model. Section III describes the proposed methods that have been used to combine GFDM with the MFSK modulation scheme, whereas in Section IV, the simulation parameters and results are presented and discussed. Finally, conclusions are presented in Section V.

II. SYSTEM MODEL OVERVIEW

A. GFDM Overiew

GFDM is one of the multicarrier modulation schemes which are proposed to address the requirements of 5G. In contrast with OFDM, GFDM can transmit up to *P* symbols, at different time slots, per each sub-carrier. An oversampling process by at least *K*, which represents the total number of the sub-carriers, is done per each sub-carrier before applying the pulse shape filtering process to decrease the OOB radiation. Non-orthogonal and orthogonal prototype filters can be used in this process which increases the flexibility of the GFDM [7]. Finally, the up-conversion process is executed before the final GFDM signal is formed by adding the sub-carrier signals simultaneously. The basic structure of the GFDM transmitter is shown in Fig.1 and the time domain of the GFDM signal can be written as:

$$x[n] = \sum_{k=0}^{K-1} \sum_{p=0}^{P-1} g_{k,p}[n] d_{k,p}, \tag{1}$$

where $d_{k,p}$ is the complex data symbol which is transmitted on the sub-carrier k and the sub-symbol p. The $g_{k,p}$ is the shifted version of the prototype filter in time and frequency and can be express as:

$$g_{k,p}[n] = g[(n - pK) mod N] e^{-j2\pi \frac{k}{K} n}, \tag{2}$$

where n is the sampling index (from 0 to N-1) and N equals to K by P. The GFDM signal, (1), can be re-expressed as:

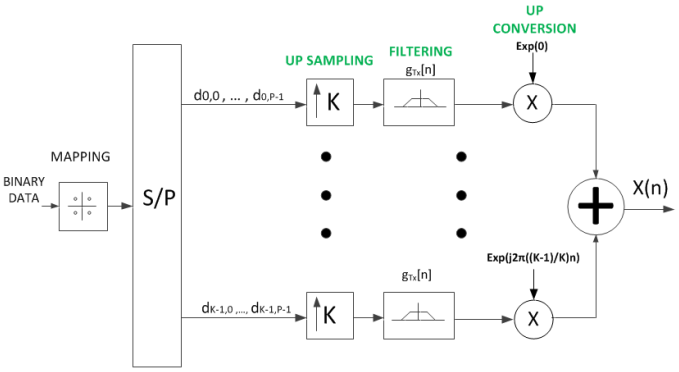

Fig. 1. The basic structure of the GFDM transmitter [8].

$$\overrightarrow{x} = A\overrightarrow{d}, \tag{3}$$

where $\overrightarrow{d}$ is the data block vector that contains N symbol and A symbolizes the transmitted matrix of the GFDM with dimension of $KP \times KP$ and its structure is mentioned by [6] as:

$$A = [\overrightarrow{g_{0,0}}.....,\overrightarrow{g_{K-1,0}},\overrightarrow{g_{0,1}}.....,\overrightarrow{g_{K-1,P-1}}] \tag{4}$$

At the receiver side, GFDM demodulation can be express as:

$$\overrightarrow{\hat{d}} = B\overrightarrow{y}, \tag{5}$$

where $\overrightarrow{y}$ is the received signal after removing the CP , B is the GFDM demodulation matrix and $\overrightarrow{\hat{d}}$ is the received data after the GFDM demodulation. Different methods to implement B can be used such as Match Filter (MF), Zero Forcing (ZF) and Minimum Mean square Error (MMSE). ZF, in which $B = A^{-1}$, is used in this paper to implement the receiver due to its simplicity. Moreover, the ZF performance loss due to the noise enhancement is zero when orthogonal pulse shape filter is used [9].

B. OFDM-MFSK Overview

The OFDM-MFSK applies a grouping of M sub-carriers, in OFDM, and applies the MFSK modulation scheme to each of these subsets (groups). This type of modulation scheme permits non-coherent detection which is especially interesting for many scenarios where no channel estimation is needed such as fast fading environment case and long range communication applications [2].

The basic structure of the OFDM-based MFSK transceiver is shown in Fig. 2. The idea of this modulation type, using M=4 (OFDM-4FSK), is illustrated in Fig. 3 where the sub-carriers are grouped into subsets of four, and only one sub-carrier per each group is chosen for transmission (the solid arrow) while no energy is transmitted on the other sub-carriers in the group (the red dots). As shown in Fig. 3, $log_2(M)$ bits, 2 bits in this example, are assigned for each subset using Grey code.

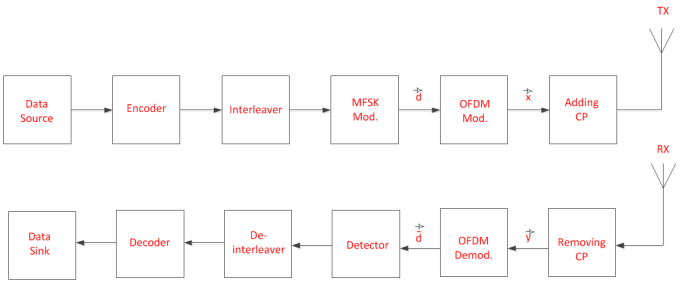

Fig. 2. Basic structure for the OFDM-based MFSK.

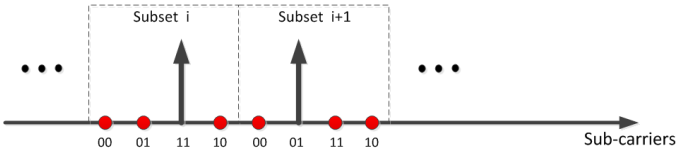

Fig. 3. Principle of OFDM-MFSK modulation (M=4).

MFSK is designed to improve receivers sensitivity at the cost of bandwidth efficiency. In this modulation scheme, the higher the value of M, the better of the sensitivity, but at the expense of lower information transmitted per unit of time. This is in contrast with bandwidth efficient modulation schemes, such as M-QAM, in which the higher the value of M, the more information is transmitted. The bandwidth utilisation for MFSK is equal to $(log_2(M)/M)$, while it is equal to $(log_2(M))$ for M-PSK/M-QAM. Table-I- illustrates the values for the bandwidth utilisation in (bit/sec./Hz) for MFSK for different values of M.

TABLE I. BANDWIDTH UTILISATION FOR THE MFSK MODULATION SCHEME.

Modulation	M=2	M=4	M=8	M=16	M=64	M=256
MFSK	1/2	1/2	3/8	1/4	3/32	1/32

Nevertheless, this leads to poor spectral efficiency, especially with the increase of M, which is main disadvantage of this modulation scheme. Some methods to improve this issue were suggested such as the hybrid transmission method which implies exploiting the phases of the occupied sub-carriers to send additional information by combining OFDM-MFSK and Differential Phase Shift Keying (DPSK) [1]. This is because non-coherent detection scheme (OFDM-MFSK) allows a random phase selection for all the sub-carriers in the transmitter side.

In multipath propagations environment (frequency selective channels), some sub-carriers can totally fade out, which leads to an error floor. Channel coding in conjunction with an interleaver is used to mitigate that. Soft decision detection is used to obtain the best performance by providing a degree of reliability for each bit to the decoder. An appropriate metric (L_j) for the j^{th} bit of a coded symbol in a transmission can be calculated based on the components of the received signal vector r_n as follows [1]:

$$L_j = max_{n \in S_j^1} \mid r_n \mid^2 - max_{n \in S_j^0} \mid r_n \mid^2, \tag{6}$$

where S_j^0 is the subset of all components indices where the codes symbols have '0' at the j^{th} digit of the bit mapping.

Thus, there is a '1' at the j^{th} digit of the bit mapping in case of S_j^1.

III. GFDM BASED MFSK (GFDM-MFSK)

Three methods where GFDM can be combined with MFSK will be discussed in the following sub-sections. The same transceiver structure, as in Fig. 2, is used in this study except that the OFDM modulator and demodulator blocks are replaced by GFDM modulator and demodulator blocks, respectively. The details of each of these methods are summarised below:

1. The Sub-Carrier Based Combination Method: In this method, the MFSK is applied on the group of sub-symbols corresponding to each GFDM sub-carrier. If P is the number of symbols per each sub-carrier, K is the number of sub-carriers and N ($P \times K$) is the number of samples in the GFDM symbol, then in this case $M = P$ (M in the MFSK =P in the GFDM). The basic structure for this case is depicted in Fig. 4 with M = 4, P = 4 and K = 4.

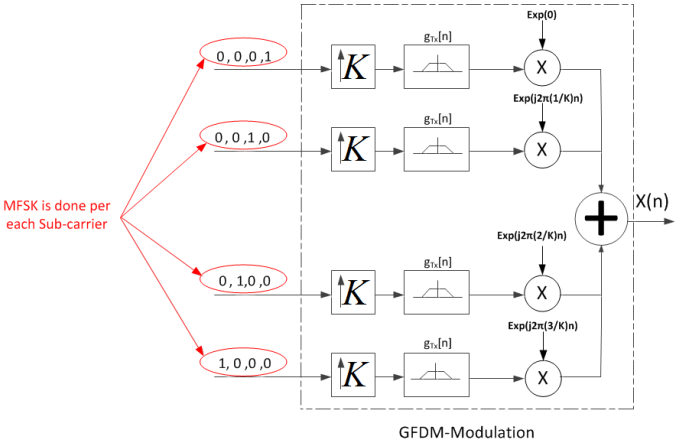

Fig. 4. GFDM-based MFSK with M=P=K=4 (Method-1) .

2. The Sub-Symbol Based Combination Method: In this case, the MFSK is applied on the group of symbols for each GFDM sub-symbol which are distributed over all active sub-carriers (e.g. the sub-symbol 'i' in each sub-carrier). In other words, in this method, M of MFSK is equal to K in GFDM. Fig. 5 shows the basic structure for this case.

3. The Mixed Sub-Carrier and Sub-Symbol Combination Method: As it is clear from the results of the previous two methods (shown in the next section) that the performance of GFDM-MFSK becomes better as the number of sub-carriers K increases (in the Rayleigh channel). Therefore, in this method there is no direct relation between the MFSK modulation parameters and the GFDM parameters. MFSK is applied for the sub-symbols that belong to the successive sub-carriers, Fig. 6 illustrates the basic structure of this method for M=K=4 and P=2. The GFDM parameters in this method, the number of sub-carriers and the number of sub-symbols per each sub-carrier, are fixed and independent on the M-size of the MFSK (they have been selected to be 128 and 2 respectively in this work).

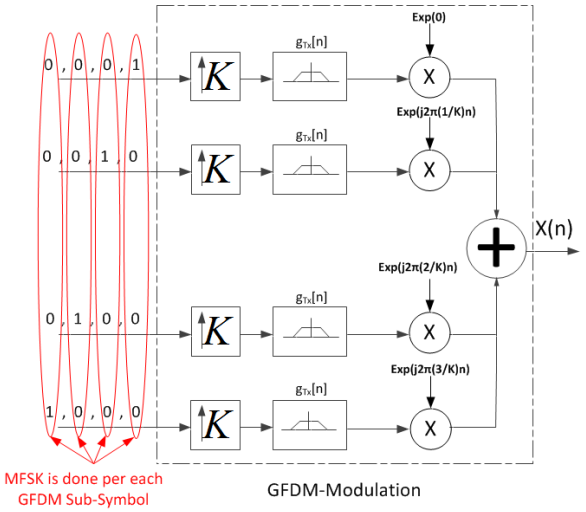

Fig. 5. GFDM-based MFSK with M=P=K=4 (Method-2) .

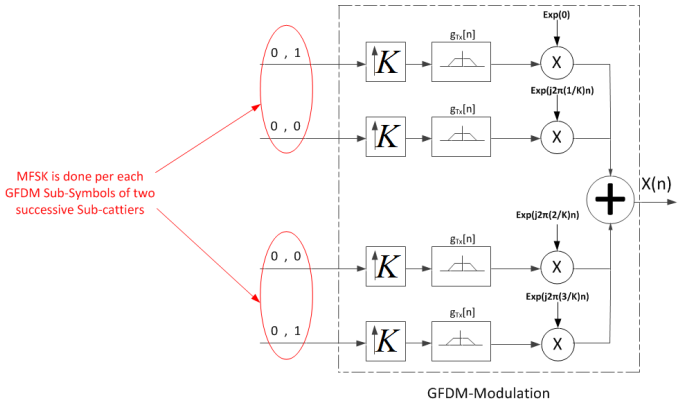

Fig. 6. GFDM based MFSK with M=K=4,P=2 (Method-3).

IV. SIMULATION PARAMETERS AND RESULT

A. Simulation Parameters.

The performance of the OFDM-MFSK and GFDM-MFSK systems was simulated using the Monte Carlo method. The simulation parameters are listed in Table II. A rate-1/2 (408,204) LDPC code was employed as a channel code with a LogMAP Sum-Product decoder [10]. To get an integer number for the OFDM and the GFDM symbols for each data packet, some zeros (N_{ZP}) were padded after encoder stage.

TABLE II. SIMULATION PARAMETERS FOR THE GFDM AND OFDM-MFSK.

Parameter	value
Input Data Block Size(N-data block)	204 bit
OFDM/GFDM Symbol Size (N)	256
Cyclic Prefix (CP) Length	32
Channel Coding	LDPC
Coding Rate (Rc)	1/2
Channel Types	-Additive White Guassian Noise (AWGN). -Wide-band Rayleigh channel with six equal power taps.
MFSK alphabet size (M)	2, 4, 8, 16, 64, 256
Prototype Filter (GFDM)	Dirichlet

The number of data symbols after the MFSK modulator

(and after zero padding) is equal to

$$N_{DataSymbol} = \left(\frac{N_{datablock}}{R_c} + N_{ZP} \right) \frac{M}{log_2 M}. \quad (7)$$

Following that, the number of OFDM (or GFDM) symbols required for a single data block can be obtained by dividing (7) by *N*. Table III summarises the results for different values of *M*.

TABLE III. NUMBER OF THE OFDM/GFDM SYMBOLS FOR DIFFERENT MFSK ALPHABET SIZE.

Alphabet Size (M)	Number of Padded Zeros (Nzp)	Number of OFDM (GFDM) Symbols Required
2	104	4
4	104	4
8	72	5
16	40	7
64	0	17
256	0	51

B. Simulation Results and Discussion

The results of three methods that proposed to combine the GFDM with the MFSK are shown and discussed below:

1. The Sub-Carrier Based Combination Method: The performance (BER versus SNR) comparison between OFDM-MFSK and GFDM-MFSK in the AWGN channel is shown in Fig. 7. Obviously, the performance of the two waveforms is fairly similar.

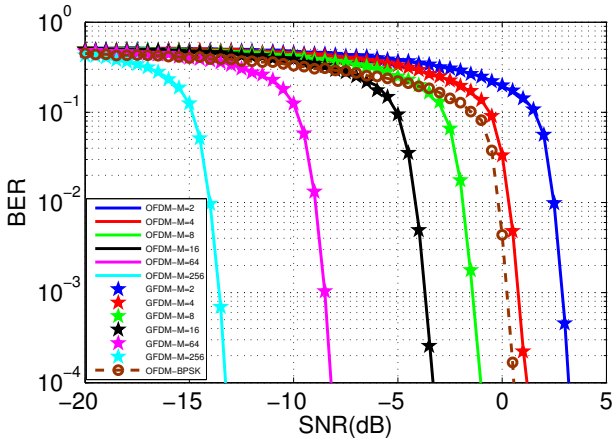

Fig. 7. BER comparison between OFDM and GFDM-MFSK (method-1) in AWGN channel.

On the other hand, Fig. 8 shows the comparison in the wide-band Rayleigh channel type. It is clear that OFDM outperforms GFDM and the difference between them increases with *M* . Less than 1 dB can be easily seen for low values of *M* ($M \leq 16$) and for high values of *M* (64 and 256), there is an error floor in GFDM. The interpretation for this result is that as *M* increases, the sub-carriers number (*K*) decreases (assuming *N* is constant and $N = K \times P$). This means that the sub-carriers bandwidth increases and it is affected more due to the frequency selectivity property of the channel. This will affect more symbols as *M* increases. Moreover, the situation becomes worse due to the absence of the equalisation stage as was previously mentioned.

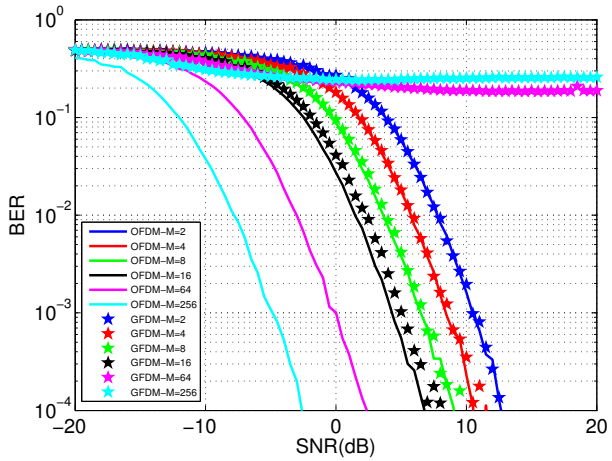

Fig. 8. BER comparison between OFDM and GFDM-MFSK (method-1) in Rayleigh channel.

2. The Sub-Symbol Based Combination Method: The performance of both waveforms in the AWGN channel model is identical and it is similar to the results of the sub-carrier based combination method (Method-1), see Fig. 7.

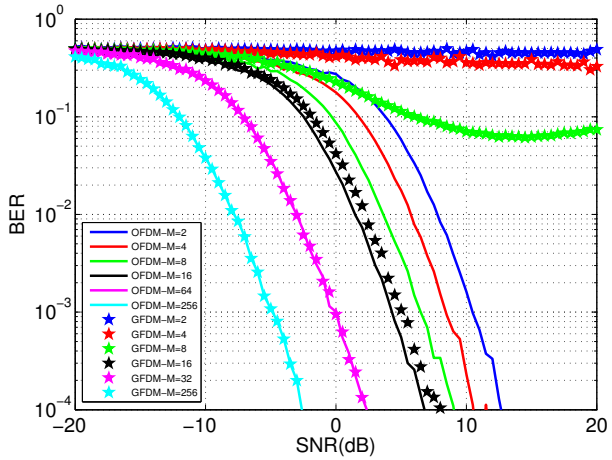

Fig. 9. BER comparison between OFDM and GFDM-MFSK (method-2) in Rayleigh channel.

Furthermore, Fig.9 depicts the BER versus SNR performance comparison in Rayleigh channel. For high values of *M* ($M \geq 64$), the performance of the two waveforms is the same, while OFDM surpasses GFDM for $M \leq 16$. Moreover, it is interesting to note that as *M* decreases, the difference between the two waveforms increases (with the SNR). The difference is less than 1 dB when $M = 16$. Additionally, the difference is increasing rapidly when $M = 8$ before the GFDM curves level at 6×10^{-2}. For *M* = 4 and 2, there is an error floor for GFDM-MFSK. The reason for this behaviour for GFDM-MFSK is as a result of decreasing *M*, which also represents the number of the sub-carriers for GFDM, the sub-carrier bandwidth increases. The sub-carriers are affected more, due to relatively large bandwidth, by the channel whose effects doesn't be equalised by the receiver (according to the specifications of the MFSK modulation type).

3. The Mixed Sub-Carrier and Sub-Symbol Combination Method: The performance of OFDM-based MFSK and GFDM-based MFSK using this method in AWGN channel is similar and the same as the previous two methods performance in AWGN, see Fig. 7.

Fig.10 shows the performance of the two waveforms in the wide-band Rayleigh channel. In contrast to the previous two methods, the results are similar for all values of M. In this case, the GFDM parameters are fixed to certain values ($P = 2, K = 128$) that do not depend on the MFSK parameter M. This means that the sub-carriers bandwidth will remain constant and also smaller compared to the low number of sub-carriers cases (less than 128).

It is interesting to note that the MFSK modulation scheme achieves a remarkable SNR gain margin that would bring significant improvements in low-rate IoT applications, such as smart meters, compared to standard OFDM or GFDM scheme at low SNR. Based on Fig.7 & Fig. 10, Table-IV shows the gain margin values for MFSK modulation scheme for different M compared to OFDM-BPSK at BER level of 1×10^{-4} in AWGN and wide-band Rayleigh channels. Please note that channel equalisation is used in OFDM-BPSK in the wide-band Rayleigh channel case. However, this is not required for OFDM-MFSK or GFDM-MFSK It is clear that gain margins of 14 & 11 dB can be achieved in the MFSK-256 modulation scheme in AWGN and Rayleigh channel respectively.

TABLE IV. GAIN MARGIN BETWEEN OFDM-BPSK & MFSK WITH DIFFERENT M VALUES IN dB.

Channel Type	M=8	M=16	M=64	M=256
AWGN	1.7	4.2	9	14
Wide-band Rayleigh	0	1.5	6	11

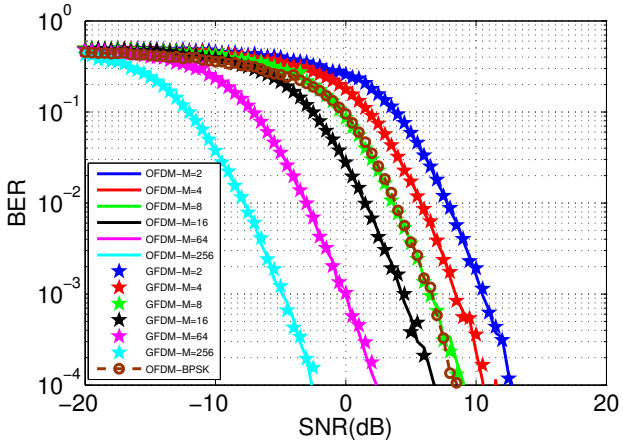

Fig. 10. BER comparison between OFDM and GFDM-MFSK (method-3) in Rayleigh channel.

V. CONCLUSION

In this paper, the GFDM-MFSK modulation scheme which is based on the combination of GFDM and MFSK was investigated. Three different methods to combine MFSK with GFDM were proposed and described. Their performance in two channel types, AWGN and wide-band Rayleigh, was evaluated, analysed and compared with that of OFDM-MFSK in the same conditions. The results show that the GFDM-MFSK performance is similar to that of OFDM-MFSK in the AWGN channel, whereas it depends on the combination method between GFDM and MFSK in the wide-band Rayleigh channel. The sub-carrier based combination method gives similar results as OFDM-MFSK at low values of M for MFSK and the performance become worse as M increases due to the decrease of the number of sub-carriers in this method. On the other hand, the sub-symbol based combination method gives similar results to OFDM-MFSK for high values of M and the performance degrades as M decreases. Eventually, the mixed sub-carrier and sub-symbol combinations method for GFDM-MFSK shows similar performance to that of OFDM-MFSK regardless of M. These results, combined with the other major advantages of the GFDM waveform such as the low OOB emission and the relaxed synchronisation requirements, will lead to a superior performance of GFDM-MFSK when compared with OFDM-MFSK. Moreover, important SNR gain margins can be obtained in MFSK modulation scheme which can provide significant improvements in low date rate 5G applications such as IoT.

ACKNOWLEDGMENT

Ghaith Al-Juboori would like to thank the Higher Committee for Education Development (HCED) in Iraq, Ministry of Oil and the University of Baghdad for sponsoring his Ph.D. studies.

REFERENCES

[1] M. Wetz, I. Peria, W. G. Teich, and J. Lindner, "Robust transmission over fast fading channels on the basis of OFDM-MFSK," *Wireless Personal Communications*, vol. 47, no. 1, pp. 113–123, 2008.

[2] M. Wetz, I. Perisa, W. G. Teich, and J. Lindner, "OFDM-MFSK with differentially encoded phases for robust transmission over fast fading channels," in *Proc. 11th International OFDM Workshop*, Conference Proceedings, pp. 313–317.

[3] Nokia, "LTE Evolution for IoT Connectivity," December-2016 2016. [Online]. Available: http://resources.alcatel-lucent.com/asset/200178

[4] L. L. Hanzo, Y. Akhtman, L. Wang, and M. Jiang, *MIMO-OFDM for LTE, WiFi and WiMAX: Coherent versus Non-coherent and Cooperative Turbo Transceivers*. John Wiley Sons, 2011, vol. 26.

[5] N. Michailow, I. Gaspar, S. Krone, M. Lentmaier, and G. Fettweis, "Generalized frequency division multiplexing: Analysis of an alternative multi-carrier technique for next generation cellular systems," in *2012 International Symposium on Wireless Communication Systems (ISWCS)*, Aug 2012, pp. 171–175.

[6] N. Michailow, M. Matthe, I. S. Gaspar, A. N. Caldevilla, L. L. Mendes, A. Festag, and G. Fettweis, "Generalized frequency division multiplexing for 5th generation cellular networks," *IEEE Transactions on Communications*, vol. 62, no. 9, pp. 3045–3061, 2014.

[7] N. Michailow, M. Lentmaier, P. Rost, and G. Fettweis, "Integration of a GFDM secondary system in an OFDM primary system," in *Future Network Mobile Summit (FutureNetw), 2011*, Conference Proceedings, pp. 1–8.

[8] G. R. Al-Juboori, A. Doufexi, and A. R. Nix, "System level 5G evaluation of GFDM waveforms in an LTE-A platform," in *2016 International Symposium on Wireless Communication Systems (ISWCS)*, Conference Proceedings, pp. 335–340.

[9] I. Gaspar, L. Mendes, M. Matth, N. Michailow, A. Festag, and G. Fettweis, "LTE-compatible 5G PHY based on generalized frequency division multiplexing," in *2014 11th International Symposium on Wireless Communications Systems (ISWCS)*, Aug 2014, pp. 209–213.

[10] D. J. Mackay, "Encycloedia of sparse random graph codes." [Online]. Available: http://www.inference.eng.cam.ac.uk/mackay/codes/data.html